Deep Space Observations of Cloud Glints: Spectral and Seasonal Dependence

Tamás Várnai, Alexander Marshak, and Alexander B. Kostinski

***Abstract*— From a distance of about one-and-a-half million kilometers, the Earth Polychromatic Camera (EPIC) onboard the Deep Space Climate Observatory (DSCOVR) spacecraft takes roughly hourly images of the sunlit side of the Earth. Earlier studies showed that these images often feature sun glint from water surfaces and from ice crystals that are suspended inside clouds in a horizontal orientation. This letter draws a wider view of the earlier analyses of observed glints caused by clouds, focusing on how the appearance of these glints varies with wavelength and season. The statistical analysis of all EPIC images taken in 2017 reveals that the wavelength dependence of glints is mainly shaped by the Rayleigh scattering and gaseous absorption caused by the air above the cloud top. The analysis also reveals that the radiative impact of cloud glints displays seasonal variations that are consistent with seasonal changes in the prevalence of ice clouds that were observed independently by the Moderate Resolution Imaging Spectroradiometer (MODIS).**

***Index Terms*— Atmosphere, clouds, ice, remote sensing.**

I. Introduction

THE Earth Polychromatic Camera (EPIC) onboard the Deep Space Climate Observatory (DSCOVR) spacecraft takes frequent multispectral images of the sunlit face of the Earth [1]. EPIC takes these images from the L1 Lagrangian point, which is about one-and-a-half million kilometers from the Earth in the direction of the Sun. EPIC captures about 22 images a day from late April to early September, and about 13 images a day during the rest of the year when the spacecraft can transmit less data as it sees the ground communication station (located in Virginia, USA) for shorter (day) times. Even casual glimpses at EPIC images (for example, at https://epic.gsfc.nasa.gov/) often reveal bright colorful spots near the image center (Fig. 1). The analysis of observation geometry (solar/viewing angles) and collocated EPIC data on oxygen absorption that provides cloud height indicated that these bright spots are caused by specular reflection from ice crystals (especially plates and columns) that float inside clouds in a horizontal orientation [2]. Therefore, the bright spots are in fact sun glint from clouds, a phenomenon often called "subsun" in atmospheric optics [3], [4]. Although the initial study of such glints [2] was limited to land areas, subsequent studies showed that such glints from ice clouds are common over oceans as well [5], [6]. Glint studies over the ocean found that cloud glints are small but bright [5] and explored radiative transfer modeling to help characterize the properties of ice crystals that cause them [6], [7]. Most recently [8], cloud glints were used to gauge the accuracy of geolocation in EPIC operational products and to examine the physical processes and instrumental considerations that affect EPIC glints caused by specular reflection from small lakes.

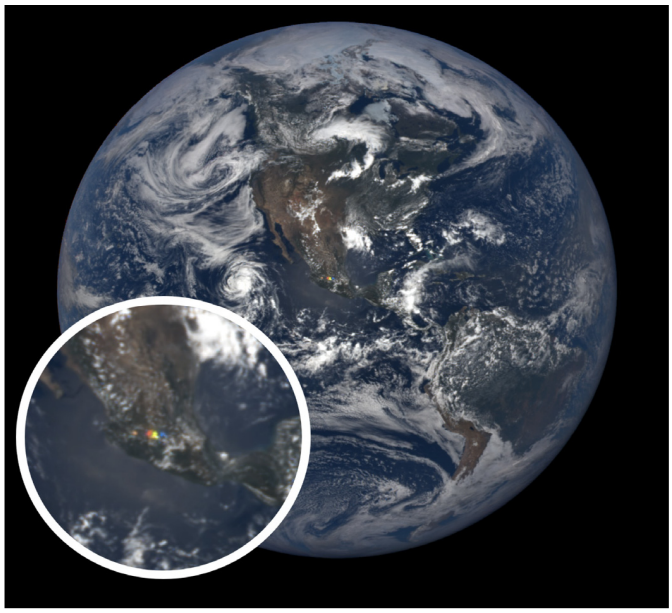

Fig. 1. Example of a sun glint caused by specular reflection from ice crystals. EPIC observed this glint over Mexico on July 4, 2018 at 16:39 coordinated universal time (UTC). The glint is centered about 200 km to the northwest from Mexico City.

This letter expands the scope of earlier analyses in two directions. First, Section II examines the question of what key factors determine the wavelength dependence of glint reflection. Understanding the spectral variations can help in a number of tasks: in relating (simulated or observed) glint data available at different wavelengths in different studies (e.g., [7], [9], [10]); in using data available only at specific discrete wavelengths for estimating whether horizontal

Manuscript received August 3, 2020; revised November 2, 2020; accepted November 17, 2020. This work was supported in part by the NASA DSCOVR Project and in part by National Science Foundation (NSF) under Grant AGS-1639868. *(Corresponding author: Tamás Várnai.)*

Tamás Várnai is with the Joint Center for Earth Systems Technology, University of Maryland, Baltimore, MD 21228 USA, and also with the NASA Goddard Space Flight Center, Greenbelt, MD 20771 USA (e-mail: varnai@umbc.edu).

Alexander Marshak is with the NASA Goddard Space Flight Center, Greenbelt, MD 20771 USA (e-mail: alexander.marshak@nasa.gov).

Alexander B. Kostinski is with the Department of Physics, Michigan Technological University, Houghton, MI 49931 USA (e-mail: kostinsk@mtu.edu).

Color versions of one or more figures in this article are available at https://doi.org/10.1109/LGRS.2020.3040144.

Digital Object Identifier 10.1109/LGRS.2020.3040144

ice crystals have significant impacts on broadband radiative energy budgets; in determining whether the observed specular reflection occurs in clouds or at the surface [2], [6]; and in obtaining information on the properties of the source—for example, on cloud type and extent, on the conditions that facilitated the presence of horizontally oriented crystals, or even on the size of horizontally oriented ice crystals [5]. Subsequently, Section III examines the seasonal variability of EPIC observations of cloud glints.

II. Wavelength Dependence

As shown in various observations of subsuns [4], sunglints from clouds appear white in red-green-blue (RGB) images in which the images of the three color channels were obtained simultaneously. The colorful image shown in Fig. 1 is thus an artifact of combining the red, green, and blue images obtained successively (with up to 4 min time difference) into an RGB image, and it was through such artifact-colorful images that the cloud glint was first discerned. As discussed in [2], the time difference between the red, green, and blue images (caused by a signature feature of EPIC, the use of a filter wheel) helps in discerning cloud glints because the rotation of the Earth continuously brings new locations to the spot where the-sun-view alignment allows EPIC to observe specular reflection—and so the intense specular reflection will appear at slightly different locations in the red, green, and blue images.

Nonetheless, cloud glints do feature some spectral variations, and the spectral features were used in [6] to distinguish cloud glints from surface glints. In contrast to [6], which analyzed the wavelength dependence of observed glint reflectances, this letter examines the wavelength dependence of the reflectance enhancements caused by sun glints (that is, by the presence of glint-causing ice crystals). We characterize the enhancement caused by specular reflection through the difference between the mean reflectance at the specular point (where EPIC views exact specular reflection from perfectly horizontal surfaces) and the mean reflectance of pixels that lie about 140 km away in any direction. These far-away pixels are outside any potential cloud glints because a 140 km distance implies a glint angle of about 3°, and earlier studies found that cloud glints are limited to glint angles less than 3° [10], [5], [8]. Cloud glints are limited to such a narrow angle-range because, according to [11]–[13], aerodynamical forces keep oriented ice crystals within a degree or so from the exact horizontal orientation.

Displaying mean values over all EPIC images acquired during 2017, Fig. 2 shows the wavelength dependence of the annual mean reflectance enhancement caused by cloud glints. We note that the results show the impact of cloud glints even though the plot is built using all (cloudy and cloud-free) pixels. This is because, as shown in [5], ocean surface glints tend to be much wider due to surface roughness, and so they cause minimal differences between points with 0° and 3° glint angles. Ultimately, Fig. 2 clearly shows the influence of two key factors shaping the wavelength dependence of enhancements: gaseous absorption and molecular scattering.

First, Fig. 2(a) shows that the enhancements drop substantially for the 688 nm and, especially, 764-nm EPIC channels,

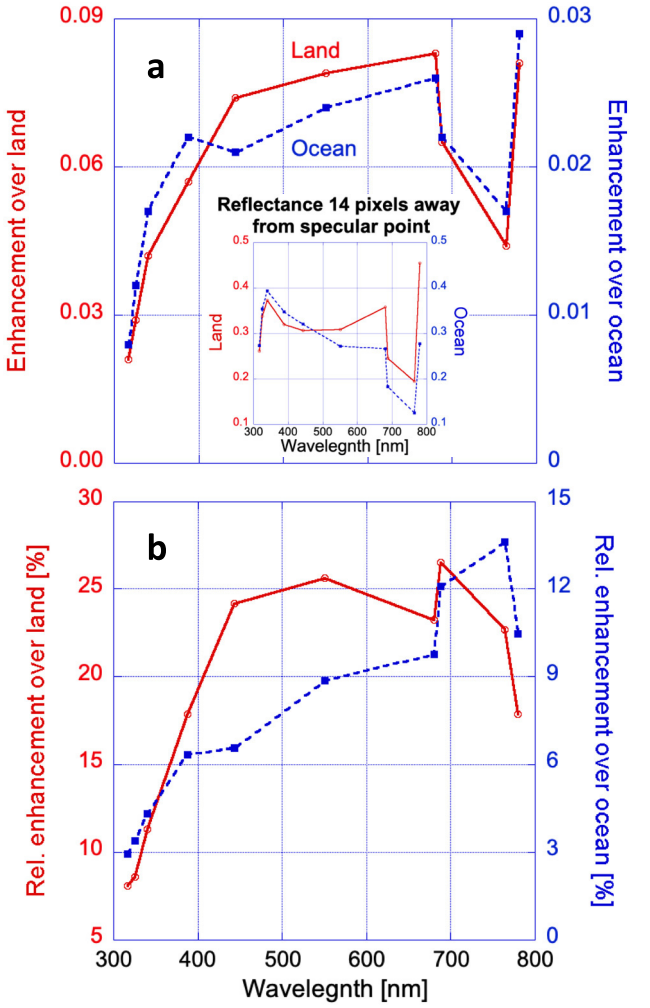

Fig. 2. Wavelength dependence of enhancements caused by specular reflection. (a) Absolute enhancements are calculated as the difference between the annual mean of reflectances observed at the specular point and 14 pixels (≈140 km) away from this point. For reference, the inset shows mean reflectances 14 pixels away from the specular point. (b) Relative enhancements calculated by dividing the absolute enhancements by the reference pixel reflectances in Panel A (in %).

which are centered on the oxygen *B* and *A* bands, respectively. The drop occurs because gaseous absorption by the air above the clouds reduces both the direct illumination of ice clouds and the amount of specularly reflected light (glint) that can pass through the above-cloud atmospheric layers. We note, however, that while the absorption reduces the magnitude of glint enhancement, it has minimal impact on the angular width of glints: Absorption changes the Full Width at Half Maximum (FWHM) by less than 4% relative to the nearby nonabsorbing EPIC bands (680 and 780 nm).

Second, Fig. 2(a) shows that glint enhancements become gradually weaker at shorter wavelengths. Much of the weakening can be attributed to Rayleigh scattering by the air above clouds, which is stronger at shorter wavelengths [14]. In addition, ozone absorption also contributes to reducing glint brightness at the shortest EPIC wavelengths (317 and 325 nm).

To complement the absolute enhancements in Fig. 2(a), Fig. 2(b) shows the spectral behavior of relative enhancements due to cloud glints. The plot shows that similar to absolute enhancements, relative enhancements also drop at the

shortest wavelengths due to the stronger Rayleigh scattering and ozone absorption. At the same time, relative enhancements are stronger—and not weaker—in oxygen absorption bands (688 and 764 nm) than in nearby nonabsorbing bands (680 and 780 nm). This is because overlying oxygen can absorb a smaller fraction of glint reflectances (coming from fairly high clouds) than reference pixel reflectances (coming mostly from lower altitudes). Also, Fig. 2(b) shows that relative enhancements over land are significantly weaker at 780 nm than at 680 nm. This can be traced back to reference pixel reflectances in Fig. 2(a) inset being much higher at 780 nm than at 680 nm due to vegetated surfaces.

We note that while the two factors mentioned above dominate, additional factors are also playing a role in shaping the observed spectral dependence. For example, the enhancement is reduced if a glint occurs over a brighter surface because if the surface is bright even without a glint, the presence of the glint makes a smaller difference.

Finally, we point out that at all wavelengths, mean enhancements are about three times stronger over land than over ocean. This is somewhat unexpected, as the analysis of POLarization and Directionality of the Earth's Reflectance (POLDER) observations did not find drastic land–sea differences in the frequency of oriented ice crystals [15], [13, Fig. 6], although cloud-aerosol lidar with orthogonal polarization (CALIOP) observations seem to suggest that the number of ice clouds warmer than −30° (where oriented crystals occur [10]) is higher over land than over ocean [10, Fig. 6(a)]. The issue of land-ocean differences is further explored in Section III.

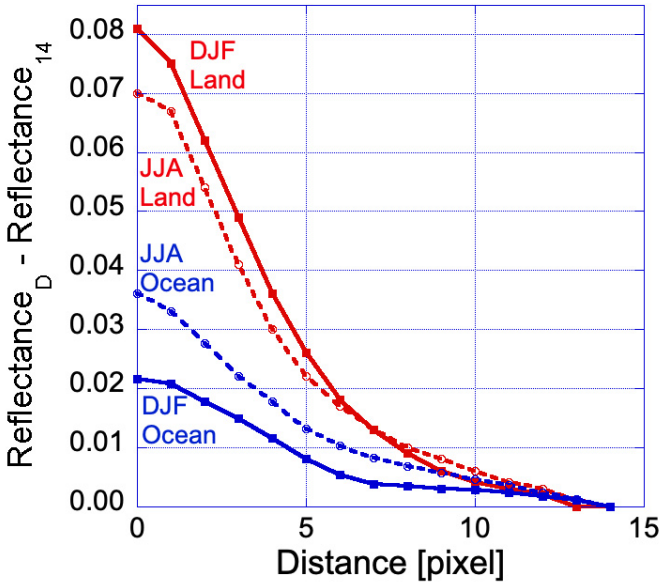

Fig. 3. Seasonal dependence of 780 nm reflectance enhancements as a function of distance (D) from the specular point. DJF means December-January-February 2017, JJA means June-July-August 2017. ReflectanceD and Reflectance14 stand for the mean reflectances at distances D and 14 pixels from the specular point, respectively.

III. Seasonal Dependence

This section examines seasonal changes in the reflectance enhancements caused by cloud glints. While most previous analyses combined glint or oriented ice crystal data from several seasons or full years, an analysis of POLDER data found significant seasonal changes in the prevalence of specular reflection from horizontally oriented ice crystals [15, Fig. 12].

Fig. 3 shows that the glint effects observed by EPIC also display significant seasonal variations, but the sign of these variations is just the opposite of those observed by POLDER: Over land, the maximum is in June for POLDER but in December-January-February (DJF) for EPIC, whereas over the ocean, the maximum is in January for POLDER but in June-July-August (JJA) for EPIC.

The difference likely comes from POLDER sampling all latitudes, whereas EPIC can observe glint in a latitude range that migrates with the seasons [2]. For example, glint can be observed by EPIC near 23° North in June, around the equator in March and September, and near 23° South in December. This is because DSCOVR is close to the Earth–Sun line, and so it can observe specular reflection at points where the solar (and viewing) zenith angle is less than about 5°—and the location of such points changes with the season due to the tilt of the Earth axis. A consequence of this migration is that in any part of the year, EPIC can observe cloud glints at tropical locations that are experiencing their wet (summer) season, whereas the POLDER statistics also include data from the local dry (winter) season and from higher latitudes. This implies that in Fig. 3, all data for the (dashed) JJA curves come from the Northern Hemisphere, all data for the (solid) DJF curves come from the Southern Hemisphere, and all curves represent data from local wet (summer) seasons. As a result, Fig. 3 shows a combination of latitudinal and seasonal dependencies. We note that March-April-May (MAM) enhancements are closer to the JJA enhancements seen in Fig. 3, whereas the September-October-November (SON) enhancements are closer to the DJF ones (not shown). This behavior is consistent with the latitude range of specular points during MAM (SON) partially overlapping with the range for JJA (DJF) (see left panel of Fig. 2 in [2]).

To better understand the seasonal changes in EPIC cloud glint effects in Fig. 3, Fig. 4 shows seasonal average ice cloud amounts observed by the Moderate Resolution Imaging Spectroradiometer (MODIS). The ice cloud fractions at typical latitudes for EPIC glint observations in DJF and JJA are highlighted by black and red stars, respectively. In agreement with the EPIC glint behavior in Fig. 3, the difference between black and red stars is opposite over land and ocean, indicating a maximum in DJF over land and in JJA over ocean.

Over land, a key factor in causing the higher amount of ice clouds and larger glint enhancements in DJF than in JJA is that that in DJF, ice clouds associated with wet season deep convection are extensive and spread far south over Africa, South America, and Australia, whereas in JJA, deep convection associated with the West African monsoon is less extensive [17], and ice clouds rarely spread north far enough to reach the latitude zone where EPIC can observe glint over the Sahel and Sahara [16, Fig. 9(c)], [18, Fig. 6].

Over the ocean, the seasonal cycle is reversed because, in DJF, ice clouds barely reach the latitude zone where

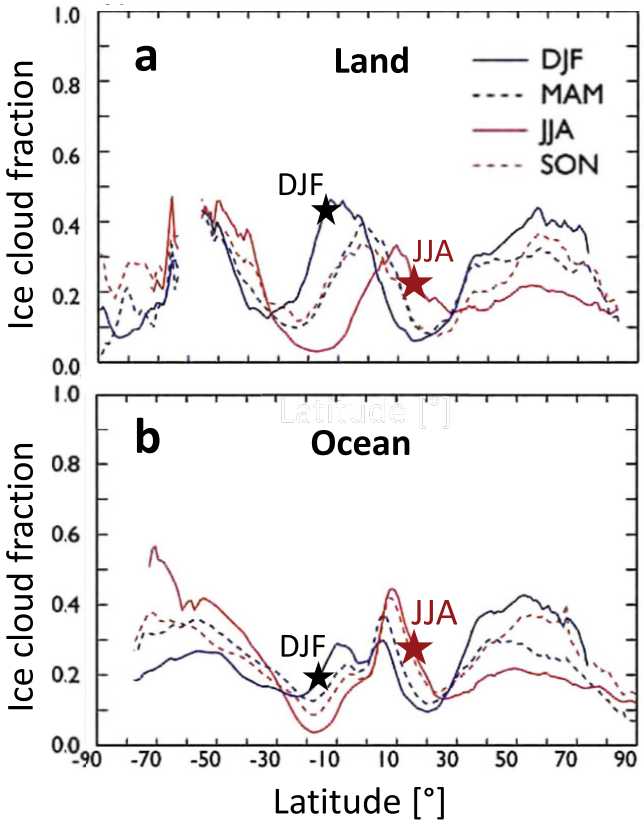

Fig. 4. MODIS data on seasonal variations in zonal mean ice cloud cover. (a) Land. (b) Ocean. Black and red stars highlight typical latitudes where EPIC can observe glint in DJF and JJA, respectively. The figure is based on Fig. 10 of [16].

EPIC can observe glints over the western Indian and western Pacific Oceans, whereas in JJA, ice clouds move north to reach this latitude zone over both the Indian and the western Pacific Oceans [16, Fig. 9(a)] and Fig. 1 in [19]). (Over the Atlantic and eastern Pacific Oceans, ice clouds remain close to the near-equator position of the Inter Tropical Convergence Zone (ITCZ) throughout the year.)

While the seasonal cycles of MODIS ice cloud amounts and EPIC cloud glints are quite similar, we note that the relationship between the total ice cloud amount and the amount of glint-producing, horizontally oriented ice crystals is somewhat tenuous. This is because most horizontal crystals occur in ice clouds warmer than −30 °C and few occur in colder, higher ice clouds [10]. One result of this is that even though in JJA the ice cloud amounts in Fig. 4 are slightly higher over ocean than over land, the glint enhancements in Fig. 3 are higher over land than over ocean. One reason for this is the very cold average cloud top temperatures over the tropical western Pacific Ocean and northeastern Indian Ocean [16, Fig. 8(a)], which implies that many ice clouds there are too cold (below −30 °C) to contain horizontally oriented crystals. One factor facilitating a higher concentration of oriented crystals in ice clouds over land may be that relatively lower humidity and higher surface temperature (more characteristic to continental regions than oceanic ones) tends to reduce the altitude and size of anvil clouds [20], [21]; indeed, the study [22] found that anvils are smaller and occur at lower altitudes over Africa and South America than over the Indian and western Pacific Oceans. Anvils being lower and smaller over land may mean that they are warmer (and can contain more oriented crystals) and obscure less of the underlying convective clouds that are warmer and thus may contain oriented ice crystals.

IV. Conclusion

Analyzing all EPIC images taken during 2017, this letter discussed spectral and seasonal variations in the sun glint caused by specular reflection from ice crystals that float in clouds at a horizontal orientation.

Because the radiative properties of large ice crystals are relatively constant in the ultraviolet-visible wavelength range, we found that the main cause of spectral variations lies in the atmosphere above clouds. In particular, glint effects become weaker when above-cloud air dampens them through Rayleigh scattering (especially at shorter wavelengths) or through absorption by ozone or oxygen. This implies that the most important factor in determining glint spectral variations is the amount of air above clouds—which, in turn, depends mainly on cloud altitude.

The results also revealed that EPIC observations of cloud glints show distinct seasonal variability over both land and ocean, but with an opposite direction: The glint signal reaches maximum in DJF over land and in JJA over ocean. This land–sea difference is likely related to the different seasonal migration of tropical convection and the different altitude and extent of anvil clouds.

Overall, the results presented in this letter expand the characterization of sun glint caused by horizontally oriented ice crystals floating in clouds. Ultimately, the analysis of EPIC observations of cloud glints may also help in interpreting glint observations taken by other instruments, such as the recently launched Hyper-Angular Rainbow Polarimeter (HARP).

References

[1] A. Marshak *et al.*, "Earth observations from DSCOVR EPIC instrument," *Bull. Amer. Meteorolog. Soc.*, vol. 99, no. 9, pp. 1829–1850, Sep. 2018, doi: 10.1175/BAMS-D-17-0223.1.

[2] A. Marshak, T. Várnai, and A. Kostinski, "Terrestrial glint seen from deep space: Oriented ice crystals detected from the lagrangian point," *Geophys. Res. Lett.*, vol. 44, no. 10, pp. 5197–5202, May 2017, doi: 10.1002/2017GL073248.

[3] D. K. Lynch, "Atmospheric halos," *Sci. Amer.*, vol. 238, no. 4, pp. 144–153, 1978.

[4] G. P. Können, "Rainbows, halos, coronas and glories: Beautiful sources of information," *Bull. Amer. Meteorolog. Soc.*, vol. 98, no. 3, pp. 485–494, Mar. 2017, doi: 10.1175/BAMS-D-16-0014.1.

[5] T. Varnai, A. B. Kostinski, and A. Marshak, "Deep space observations of sun glints from marine ice clouds," *IEEE Geosci. Remote Sens. Lett.*, vol. 17, no. 5, pp. 735–739, May 2020, doi: 10.1109/LGRS.2019.2930866.

[6] J.-Z. Li *et al.*, "Study of terrestrial glints based on DSCOVR observations," *Earth Space Sci.*, vol. 6, no. 1, pp. 166–173, Jan. 2019, doi: 10.1029/2018EA000509.

[7] V. Noel and H. Chepfer, "Study of ice crystal orientation in cirrus clouds based on satellite polarized radiance measurements," *J. Atmos. Sci.*, vol. 61, no. 16, pp. 2073–2081, 2004, doi: 10.1175/1520-0469(2004)061<2073:SOICOI>2.0.CO;2.

[8] A. Kostinski, A. Marshak, and T. Várnai, "Deep space observations of terrestrial glitter," *Earth Space Sci.*, accepted for publication

[9] Y. Takano and K.-N. Liou, "Solar radiative transfer in cirrus clouds. Part II: Theory and computation of multiple scattering in an anisotropic medium," *J. Atmos. Sci.*, vol. 46, no. 1, pp. 20–36, Jan. 1989.

[10] V. Noel and H. Chepfer, "A global view of horizontally oriented crystals in ice clouds from cloud-aerosol lidar and infrared pathfinder satellite observation (CALIPSO)," *J. Geophys. Res.*, vol. 115, May 2010, Art. no. D00H23, doi: 10.1029/2009JD012365.

[11] D. K. Lynch, S. D. Gedzelman, and A. B. Fraser, "Subsuns, bottlinger's rings, and elliptical halos," *Appl. Opt.*, vol. 33, no. 21, pp. 4580–4589, 1994, doi: 10.1364/AO.33.004580.

[12] J. I. Katz, "Subsuns and low Reynolds number flow," *J. Atmos. Sci.*, vol. 55, no. 22, pp. 3358–3362, 1998, doi: 10.1175/1520-0469(1998)055<3358:SALRNF>2.0.CO;2.

[13] F.-M. Bréon and B. Dubrulle, "Horizontally oriented plates in clouds," *J. Atmos. Sci.*, vol. 61, no. 23, pp. 2888–2898, 2004, doi: 10.1175/JAS-.3309.1.

[14] B. A. Bodhaine, N. B. Wood, E. G. Dutton, and J. R. Slusser, "On Rayleigh optical depth calculations," *J. Atmos. Ocean. Technol.*, vol. 16, no. 11, pp. 1854–1861, 1999, doi: 10.1175/1520-0426(1999)016<1854:ORODC>2.0.CO.2.

[15] H. Chepfer, G. Brogniez, P. Goloub, F. M. Bréon, and P. H. Flamant, "Observations of horizontally oriented ice crystals in cirrus clouds with POLDER-1/ADEOS-1," *J. Quant. Spectrosc. Radiat. Transf.*, vol. 63, nos, 2–6, pp. 521–543, 1999, doi: 10.1016/S0022-4073(99)00036-9.

[16] M. D. King, S. Platnick, W. P. Menzel, S. A. Ackerman, and P. A. Hubanks, "Spatial and temporal distribution of clouds observed by MODIS onboard the terra and aqua satellites," *IEEE Trans. Geosci. Remote Sens.*, vol. 51, no. 7, pp. 3826–3852, Jul. 2013, doi: 10.1109/TGRS.2012.2227333.

[17] N. C. G. Hart, R. Washington, and R. I. Maidment, "Deep convection over Africa: Annual cycle, ENSO, and trends in the hotspots," *J. Climate*, vol. 32, no. 24, pp. 8791–8811, Dec. 2019, doi: 10.1175/JCLI-D-19-0274.1.

[18] C. J. Stubenrauch, S. Cros, A. Guignard, and N. Lamquin, "A 6-year global cloud climatology from the atmospheric InfraRed sounder AIRS and a statistical analysis in synergy with CALIPSO and CloudSat," *Atmos. Chem. Phys.*, vol. 10, no. 15, pp. 7197–7214, Aug. 2010, doi: 10.5194/acp-10-7197-2010.

[19] H. Cheng, A. Sinha, X. Wang, F. W. Cruz, and R. L. Edwards, "The global paleomonsoon as seen through speleothem records from Asia and the Americas," *Climate Dyn.*, vol. 39, no. 5, pp. 1045–1062, Sep. 2012, doi: 10.1007/s00382-012-1363-7.

[20] M. D. Zelinka and D. L. Hartmann, "The observed sensitivity of high clouds to mean surface temperature anomalies in the tropics," *J. Geophys. Res., Atmos.*, vol. 116, no. D23, Dec. 2011, Art. no. D23103, doi: 10.1029/2011JD016459.

[21] S. Bony *et al.*, "Thermodynamic control of anvil cloud amount," *Proc. Nat. Acad. Sci. USA*, vol. 113, no. 32, pp. 8927–8932, Aug. 2016, doi: 10.1073/pnas.1601472113.

[22] J. Yuan and R. A. Houze, "Global variability of mesoscale convective system anvil structure from A-train satellite data," *J. Climate*, vol. 23, no. 21, pp. 5864–5888, Nov. 2010, doi: 10.1175/2010JCLI3671.1.